Journal of Photochemistry and Photobiology A: Chemistry 224 (2011) 62–67

Contents lists available at SciVerse ScienceDirect

Journal of Photochemistry and Photobiology A: Chemistry

journal homepage: www.elsevier.com/locate/jphotochem

Effect of solvent polarity on photophysical parameters of 3-aminoflavone

Łukasz Wiśniewski[a], Irena Deperasińska[b], Bogusława Żurowska[a], Anna Szemik-Hojniak[a,*]

[a] Faculty of Chemistry, University of Wroclaw, Joliot-Curie 14 st; 50-383 Wroclaw, Poland
[b] Institute of Physics, Pol. Acad. of Sciences, Al.Lotników 32/46, 02-668 Warsaw, Poland

ARTICLE INFO

Article history:
Received 1 July 2011
Received in revised form 7 September 2011
Accepted 10 September 2011
Available online 16 September 2011

Keywords:
3-Amino flavone
Fluorescence
DFT and TD DFT calculations
PCM model
Electron transfer
Lifetimes
CT states
Triplet states

ABSTRACT

Photophysical behavior of 3-amino flavone (3AF) in different media has been studied using steady state and time-resolved fluorescence spectroscopy in combination with DFT and TD DFT B3LYP/6-31G (d,p) calculations involving the ground and the excited state geometry optimization. Comparison of experimental solvatochromic shifts with the calculated energies in different solvents (PCM model) allows to conclude that the excited state of 3AF, corresponding to the $\pi \rightarrow \pi^*$ ($S_0 \rightarrow S_1$) transition, has a partial CT nature. The lifetime and quantum efficiency measurements in function of solvent polarity shown that in weakly polar solvents the radiationless rate constant is very high. On the basis of TD DFT calculations for singlet and triplet state distribution in different environments (PCM model) we hypothesize that in weakly polar solvents the intersystem crossing may be a prevailing relaxation process.

1. Introduction

The flavonoids are the natural, biologically active systems occurring in plants. Both the original products and their synthetic derivatives demonstrate a large scale of important pharmacological applications including antioxidant, cytostatic, anti-inflammatory or anticancer properties [1–3]. They also play an important protective action with respect to the cell membranes preventing photosensitized products from damages [4].

The flavones, being a sub group of flavonoids, besides their biological activity they are also interesting objects because of their complex photophysical properties including excited state intramolecular proton (ESIPT) and/or electron transfer (ET) processes. The ESIPT occurring along the O–H···O hydrogen bond has been analyzed in numerous examples of 3-, 5-, or 7-hydroxyflavones [5–7]. In either of them the effect of the solvent polarity on deactivation pathways of excited molecules is clearly visible. Usually, excitation of 3HF in the gas phase or in apolar solvent conditions leads to a single, red shifted tautomeric green fluorescence (520 nm) while in alcohols or in strongly polar solvents a double luminescence is observed. The blue 380–460 nm emission is assigned to the normal hydrogen bonded "N" form and the green emission in the range 510–570 nm to the tautomeric "T" form [8]. Surprising results were obtained from experimental emission spectra of 3-hydroxyflavone in supercritical CO_2 [9]. They show that the fluorescence of the normal, hydrogen bonded form, may be observed not only from the S_1 but also from the S_2 state (27,000 and 32,000 cm^{-1}, respectively) although the tautomeric emission occurs, as usually, in the green spectral region [9].

Remarkable solvent- polarization-dependent ESIPT reaction dynamics involving the charge transfer (CT) character of the emissive state was observed due to a substitution of the phenyl ring of 3HF with di-alkylamino groups, as strong electron donors [10–12]. A good example of an ultrafast, adiabatic ESIPT was found in diethylamino—derivative of 3-hydroxyflavone (DEA-3HF) [13], which in apolar solvents shows a single tautomeric emission band (560 nm) with the Stokes shift of ~8000 cm^{-1} whereas in polar solvents both the normal (N*) and the tautomeric (T*) transitions are observed.

Recently, the CT nature of the fluorescence emission has also been stated in daidzein, a model isoflavone [14] where the OH group was substituted in position 4′ of the phenyl ring and in position 7 of the chromone part. Daidzein is not emitting in polar acetonitrile while a weak emission (460 nm) was observed in acidic water environment. Its CT character is due to the shift of charge from the phenyl to the chromone ring what was confirmed both by a large Stokes shift (1.4 eV) and a significant change in the dipole moment ($\Delta\mu$ = 3.23 D).

The major goal of this study is to gain a better insight into photophysical properties of the low-lying electronic excited states of

* Corresponding author. Tel.: +48 71 3757 366.
E-mail address: anna.szemik@chem.uni.wroc.pl (A. Szemik-Hojniak).

1010-6030/$ – see front matter © 2011 Elsevier B.V. All rights reserved.
doi:10.1016/j.jphotochem.2011.09.007

3-amino flavone (3AF) in solvents of different polarity by employing the steady state and time resolved fluorescence measured by the time-correlated single-photon counting (TCSPC) technique. In the final step experimental results are compared to the calculated absorption and emission spectra (PCM model) of 3AF.

2. Experimental

2.1. Materials

The solvents used in absorption and emission experiments, i.e. iso-octane (IO), hexane (HEX), di-ethyl eter (Et–O–Et), ethyl acetate (EtAc), tetrahydrofurane (THF), ethyl alcohol (EtOH), acetonitrile, and glycerol were of spectroscopic grade and used fresh as purchased (Merck, Uvasol). Water was of HPLC grade. The synthesis, purification and identification of 3AF was described elsewhere [15].

2.2. Characterization

Electronic absorption spectra in solution were recorded on CARY-50 UV–VIS (Varian) spectrometer at the concentration of about 10^{-6} M. Emission spectra were recorded on FLS920 combined fluorescence lifetime and steady state spectrometer (Edinburgh Instruments Ltd) using as excitation source Xe900, 450 W steady state xenon lamp (ozone free) with computer controlled excitation shutter and with spectral bandwidth of ≤5 nm for both excitation and emission spectra. Luminescence was detected using a red sensitive (185–850 nm) photomultiplier tube (R928-Hamamatsu) in a Peltier cooled housing. For emission spectra the optical density was kept at ∼0.2 (path length 1 cm) to avoid re-absorption and inner filter effects. Spectra were corrected for detector response and excitation source. The concentration of the solutions was of the order 10^{-6} M. Fluorescence quantum yield was estimated using quinine sulphate in 0.05 M H_2SO_4 solution ($\varphi_F = 0.55$) as a standard [16]. Fluorescence lifetimes were measured in solution (10^{-6} M) using TCSPC option of FSL920 set-up (Edinburgh Instruments Ltd.). Excitation was provided by nF900 nitrogen filled nanosecond flashlamp under computer control, with typical pulses width 1 ns, and pulse repetition rate typical 40 kHz and possibility of measuring decays from 100 ps to 50 μs. Data acquisition ensured plug-in PC card with time channels per curve up to 4096. A Hamamatsu (R928-Hamamatsu) in Peltier Cooled Housing was used as detector.

Calculations were performed on DFT B3LYP/6-31G(d,p) and TD DFT B3LYP/6-31G (d,p) level of theory. The ground state (S_0) structure optimization of 3AF was performed by means of the first method. The excited (S_1) state optimization along with the energy and oscillator strength calculations for electronic transitions between the S_0 and S_1 states of 3AF both in the gas and the liquid phase were calculated by the second method. The solvent polarity has been involved in the framework of PCM model. For all calculations, the GAUSSIAN 09 [17] package of programs was employed.

3. Results and discussion

3.1. Molecular structures of 3AF in the ground (S_0) and excited (S_1) electronic state

The 3AF studied here, as opposed to a broad range of known 3-hydroxy flavones [7,13] in position 3, relative to the >C=O group, has an amino group.

The X-ray structure of 3AF (Fig. 1.) was reported and described elsewhere [15]. Its structural parameters (atom coordinates, bond lengths, valence angles, dihedral angles, etc.) are deposited at the Cambridge Crystallographic Data Center CCDC No. 637639.

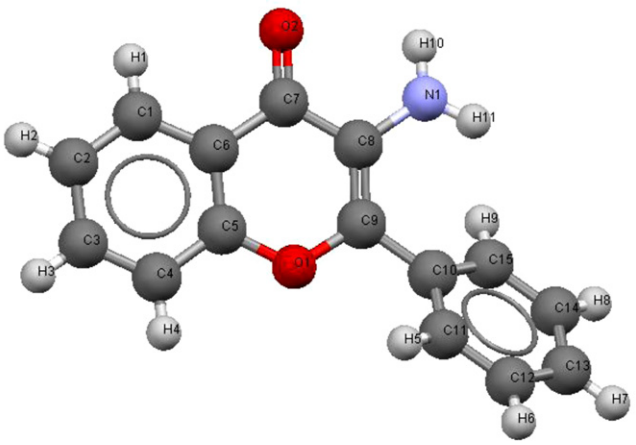

Fig. 1. Crystal structure of 3AF with atom numbering [15] (taken from the Cambridge Crystallographic Data Center CCDC No. 637639).

Accordingly to these data, both the chromone and the phenyl ring are planar although they are twisted one to another about 40.66(4)° [15]. The crystal packing of 3AF is stabilized by a network of weak intermolecular C–H···O [3.229(3) Å] hydrogen bonds. In this compound, the intramolecular N–H···O hydrogen bond between the nitrogen atom of the amino group and the oxygen atom of the carbonyl group was not found. Hence, contrary to numerous examples of ESIPT processes in 3-hydroxy flavone derivatives, the excited state photoinduced electron transfer may be expected in 3AF, instead.

Experimental data are correctly reproduced by the calculations and the bond lengths around the amino and the carbonyl group are very close to them. Generally, comparison of all calculated parameters of isolated 3AF molecule to those experimentally obtained in the solid state confirms precision of the DFT B3LYP/6-31G(d,p) method.

The most important structural parameters of 3AF in the ground (S_0) and excited electronic (S_1) state are gathered in Table 1.

They show that despite the shortening of the CN bond (0.04 Å) and the NH···O distance (0.07 Å) combined with the change in the valence NHO angle (109.9°), the intramolecular hydrogen bond of the NH···O type is not formed. Hence, in the case of 3AF, the ESIPT process can not be expected.

3.2. Absorption and emission spectra

3.2.1. Experimental spectra

The room temperature absorption, fluorescence and excitation fluorescence spectra of 3AF have been measured in solvents of different polarity and hydrogen bonding abilities. As an example, such spectra in iso-octane (along with simulated absorption and emission spectra, see the following chapter) are presented in Fig. 2.

Table 1
Chosen experimental [15] and DFT [B3LYP/6-31G(d,p)] calculated ground state (S_0) as well as [CIS/6-31G(d,p)] calculated excited state (S_1) geometrical parameters of 3AF.

Parameter	Crystal (exp)	S_0	S_1
d(C8–N1)Å	1.396(2)	1.39	1.35
d(C7–O2) Å	1.244(2)	1.24	1.25
d(C9–C10) Å	1.473(3)	1.47	1.45
d(C5–O1) Å	1.372(2)	1.34	1.35
d(O1–C9) Å	1.382(2)	1.35	1.38
[C8–C9–C10–C15]°	40.66(4)°	29.4°	28.4°
[N1–H10–O2]°	101.22°	108.5°	109.9°
d(N1···O2) Å	2.684(2)	2.67	2.61

Table 2
Room temperature electronic absorption and emission properties of 3AF in various solvents.

	ε	Abs* (nm)	Fl* (nm)	Stokes shift (cm^{-1})	Lifetime (ns)	Q_F	k_r (s^{-1})	k_{nr} (s^{-1})
Hexane	1.88	359	425	4326	1.13	0.067	5.93E+07	8.26E+08
3MP	1.94	359	425	4326	1.20	0.09	7.30E+07	7.60E+08
Et–O–Et	4.32	364	453	5395	3.75	0.27	7.20E+07	1.90E+08
$CHCl_3$	4.81	364	450	5250	4.66	0.27	5.79E+07	1.57E+08
EtAc	6.11	365	456	5460	4.65	0.26	5.62E+07	1.61E+08
THF	7.52	369	466	5641	4.92	0.27	5.49E+07	1.48E+08
EtOH	24.55	366	480	6489	5.07	0.29	5.72E+07	1.40E+08
AN	35.95	372	495	6979	5.21	0.32	6.12E+07	1.38E+08
Glycerol	42.5	358	490	7525	–	–	–	–
H_2O	78.3	353	490	7920	2.79	0.12	4.3E+07	3.2E+08

More detailed experimental data on photophysical parameters of 3AF in various solvents are collected in Table 2.

In Fig. 2, first absorption band and the fluorescence band are broad and structureless, being each other mirror images. Excitation spectra of 3AF properly reproduce absorption spectra, implying that the excited molecule shows no sign of photochemistry and its excited state deactivation processes lead directly to the ground state.

In polar solvents absorption spectra of 3AF (Table 2) are slightly red shifted (359 nm in hexane and 369 nm in THF) whereas a hipsochromic shift, appears in water (353 nm) and alcohols (358 nm in glycerol) due to the formation of intermolecular hydrogen bonds. Spectral shifts are especially distinct in the fluorescence spectra. With an increasing solvent polarity the peaks maxima are more readily shifted towards longer wavelengths than in absorption (iso-octane, 425 nm; water, 490 nm). The last two entries of Table 2 present the radiative and nonradiative rate constants, derived from the estimated quantum yields and the measured fluorescence lifetimes. An interesting fact is that the value of the radiationless rate constants in iso-octane or hexane (~8.0E+08) is much higher than in polar solvents. To interpret the experimental spectra of 3AF and the effect of solvent polarity, we shall employ the results of quantum-chemical calculations, which are outlined below.

3.2.2. Simulated spectra

The TD DFT calculated absorption spectrum of 3AF in the gas phase, presented in Fig. 2, precisely reproduces the experimental spectrum in iso-octane. It shows that the maximum of the allowed (f = 0.241) first absorption band (27,231 cm^{-1}) is in a good agreement with respect to the experiment (27,855 cm^{-1}).

The calculation results reflect the most important features of the experimental spectrum of 3AF, both in terms of the overall spectral shape and the energy maxima. On the basis of the calculated oscillator strengths we find that the first absorption band is build upon a single, most intensive electronic transition. The transition is well separated from the higher energetic bands (in the energetic scale) that represent only a weakly allowed transitions.

The TD DFT eigenvectors analysis shows that the optical $S_0 \rightarrow S_1$ transition is described by the ($\pi\pi^*$) HOMO → LUMO electronic configuration (see Fig. 3). Fig. 3 demonstrates, *inter alia*, that in this transition, the charge transfer takes place on excitation from the electron rich amino group to the electron deficient carbonyl group and the aromatic ring of the chromone system. The lower part of this figure shows how the electron density shifts from the electron donor to the electron acceptors and how it is distributed after excitation.

On this basis, one can conclude that the S_1 state of 3AF, corresponding to the $\pi \rightarrow \pi^*$ ($S_0 \rightarrow S_1$) transition, has only a partial CT nature.

The calculated energetic relationships between the ground and excited state optimized structures of 3AF are depicted in the diagram of Fig. 4. The figure shows electronic energy of the $S_0 \rightarrow S_1{}^{FC}$ transition (absorption), $S_1 \rightarrow S_0{}^{FC}$ transition (fluorescence), the

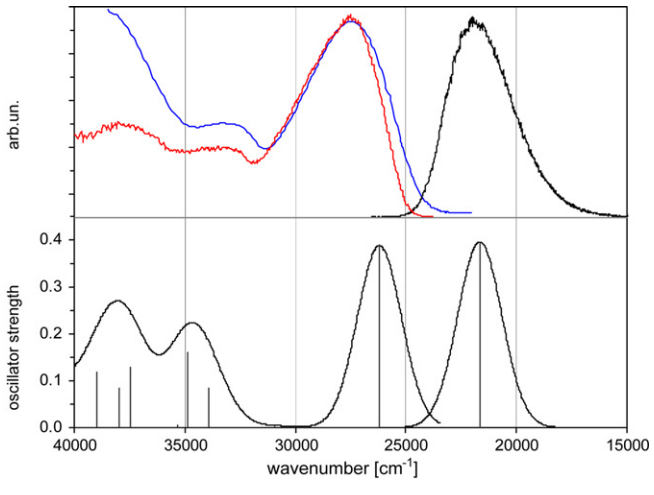

Fig. 2. (At the top) The normalized absorption, fluorescence and excitation fluorescence spectra of 3AF in iso-octane solution (concentration about 10^{-5} M; exc. 365 nm; em. 456 nm). (At the bottom) The simulated absorption and fluorescence spectrum of 3AF molecule in the same solvent (PCM model). The simulation is performed on the basis of TD DFT calculations (see text and Table 3). The vertical lines represent the calculated transition energies, their heights correspond to the calculated oscillator strengths. For spectra simulation, each of the calculated lines was convoluted with Gaussian distribution of 1300 cm^{-1} width.

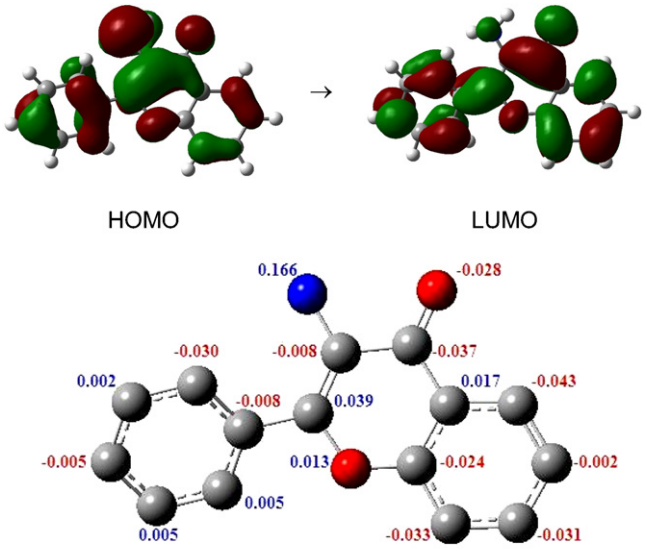

Fig. 3. The character of the $S_0 \rightarrow S_1$ transition in 3AF. (At the top) The frontier molecular orbitals of electronic configuration characterizing the $S_0 \rightarrow S_1$ transition in 3AF molecule. At the bottom, the differences in the size of the electron charge between the S_1 and S_0 states [$q(S_1) - q(S_0)$] on particular atoms of 3AF (the hydrogen atoms have been included into summation).

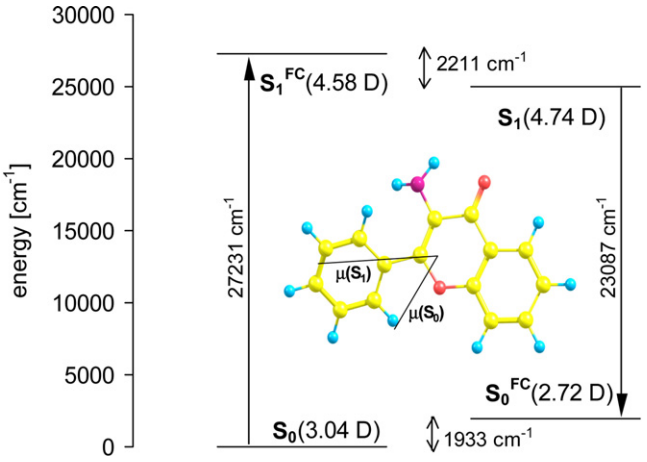

Fig. 4. The energetics of isolated 3AF molecule. The S_0 and $S_1{}^{FC}$ states indicate the ground and the lowest excited state, respectively, with the ground state optimization. The S_1 and $S_0{}^{FC}$ states—are the states corresponding to the structure optimized in the S_1 excited state. Hence, the index FC indicates the final state in perpendicular transition, i.e. the Franck–Condon state. The figure also shows electronic energy of the $S_0 \rightarrow S_1{}^{FC}$ transition (absorption), $S_1 \rightarrow S_0{}^{FC}$ transition (fluorescence), dipole moments in these states and their directions.

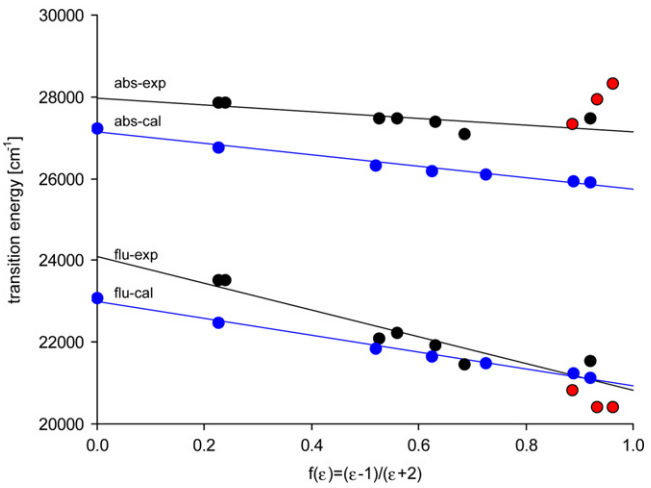

Fig. 5. Comparison of experimental absorption (abs–exp) and emission maxima (flu–exp) of 3AF in solvents of various polarity (Table 2) with TDDFT calculated energies for $S_0 \rightarrow S_1{}^{FC}$ (abs–cal) and $S_1 \rightarrow S_0{}^{FC}$ (flu–cal) transitions (Table 3) *versus* polarity function $[f(\varepsilon) = (\varepsilon - 1)/(\varepsilon + 2)]$. The dots indicate experimental or calculated values while the straight lines (determined by the linear regression method) are drawn to facilitate the assignment of individual dots to specified dependency. For solvents with a strong hydrogen bonding abilities (alcohols) the dots are clearly deviated from the straight lines.

dipole moments in these states and their directions. It takes into account that both the absorption and fluorescence processes lead to the Franck–Condon states.The significant energy difference between absorption and fluorescence maxima in the gas phase ($\sim$4000 cm^{-1}) ensures the excited state stabilization of this system, especially when the excited dipole is immersed in the polar media. The 3AF molecule has a fairly large ground state dipole moment (3.04D) that increases (4.74 D, Fig. 4) and changes its direction in the excited state. The observed changes are directly related to the charge transfer between the amino substituent and the chromone ring what in turn allows one to expect a significant solvent polarity effect on the energies of the electronic excited states in polar solvents. This can indeed be observed in the experiment (see Table 2).

By the means of the PCM model (included in the GAUSSIAN 09 package of programs [17]), we have tried to check environmental effect on the energy change, oscillator strength, and dipole moments on the $S_0 \rightarrow S_1{}^{FC}$ (absorption) and the $S_1 \rightarrow S_0{}^{FC}$ (fluorescence) transitions in various solvents. The results of calculations both for the ground (S_0) and the excited (S_1) state are demonstrated in Table 3.

As one can easily note, with increasing solvent polarity, the dipole moment clearly increases both in the ground and in the excited state. This leads to a decline in transition energies both in absorption and emission. A more detailed comparison between experiment and calculations is presented in Section 3.2.3.

3.2.3. Comparison of the calculated absorption and emission spectra with experiment

A general solvent effect results from the interactions between the solute and the solvent molecule. Such interactions lead to the energy difference between the ground and excited state and are observed in the solvent dependent spectral shifts in absorption and emission spectra.

In this chapter, a comparison between experimental spectral shifts and the appropriate calculated data is performed. For this purpose, experimental absorption and fluorescence maxima in different solvents (Table 3) are referred to TD DFT calculated the $S_0 \rightarrow S_1{}^{FC}$ and $S_1 \rightarrow S_0{}^{FC}$ transition energies (PCM model, Table 3) and demonstrated *versus* the solvent polarity function $[f(\varepsilon) = (\varepsilon - 1)/(\varepsilon + 2)]$ (Fig. 5).

The results in Fig. 5, not only facilitate the comparison of the experimental and the theoretical results, but may also refer to the Onsager model, where the solute molecule is considered to be a dipole, immersed, in a continuous medium of uniform dielectric constant [18].Measurements for 3AF were performed in various solvents (diethyl ether, ethyl acetate, THF, AN), which are frequently used to study the solvent dependent properties of the CT states. The obtained results do interplay both with the data for solvents without the hydrogen bonding abilities (as opposed to alcohols) and with the results of calculations where ability of the medium to form the hydrogen bonds do not play a role. This allows concluding that the ability of the hydrogen bonding formation in these solvents is secondary with respect to their dielectric strength.

As one can see in Fig. 5, with the exception of water, EtOH, and glycerol [the highest values of $f(\varepsilon)$ function], the points of experimental absorption and fluorescence maxima along with the calculated energies of the $S_0 \rightarrow S_1{}^{FC}$ transition for other solvents used are arranged in almost parallel lines. A slight difference observed between the slopes of presented lines for absorption and fluorescence although not a dramatic, requires a proper explanation.

We find that the use of the Onsager model, reflects a larger difference between the dipole moments determining the fluorescence dependency on the solvent polarity $[\mu(S_1) - \mu(S_0{}^{FC}) \sim 2D]$ than models used to describe absorption $[(\mu(S_1{}^{FC}) - \mu(S_0) \sim 1.7D]$ (see Table 3).

Besides that, a deviation of points between the experimental and theoretical lines can result from the fact that the calculated quantity is the electronic transition energy, as well as that the maximum of absorption is taken into account. What's more, we can say that this is due to the inaccuracy of the calculations. Neglecting, however, this quantitative discrepancy, we are able to show in this study that in a broad range of solvent polarities, a good compatibility between experiment and calculations may be achieved.

This also allows us to conclude that values of the calculated dipole moments, gathered in Table 3, are close to the real ones. One may note that with increasing solvent polarity, larger experimental spectral shifts are observed for the fluorescence than for the absorption spectra. Hence, compatibility between the calculated energy changes for the $S_1 \rightarrow S_0{}^{FC}$ transition and the fluorescence maxima is not as evident as for absorption. Also, the energy calculations performed for the molecular structure of 3AF with the excited state

Table 3
The TD DFT/B3LYP/6-31G(d,p) calculated values of transition energies (ΔE), oscillator strength (f), and dipole moments (μ) in the ground and excited state of 3AF molecule in solvents of various polarity (PCM model).

Solvent	$f(\varepsilon)$	$\Delta E(S_0 \rightarrow S_1{}^{FC})$ (cm^{-1})	Oscillator strength (f)	$\mu(S_0)$ (D)	$\mu(S_1{}^{FC})$ (D)
3AF optimized in S_0 state					
FREE	0.000	27,231	0.241	3.04	4.58
HEX	0.227	26,757	0.307	3.48	5.09
DEE	0.519	26,326	0.371	3.92	5.59
EtAc	0.624	26,190	0.390	4.06	5.75
DCM	0.726	26,097	0.407	4.18	5.88
ACN	0.920	25,911	0.436	4.39	6.11
Solvent	$f(\varepsilon)$	$\Delta E(S_1 \rightarrow S_0{}^{FC})$ (cm^{-1})	Oscillator strength (f)	$\mu(S_0{}^{FC})$ (D)	$\mu(S_1)$ (D)
3AF optimized in S_1 state					
FREE	0.000	23,088	0.255	2.72	4.74
HEX	0.227	22,469	0.327	3.11	5.13
DEE	0.519	21,840	0.397	3.49	5.55
EtAc	0.624	21,649	0.418	3.61	5.67
DCM	0.726	21,480	0.436	3.71	5.79
ACN	0.920	21,130	0.466	3.89	5.99

The $f(\varepsilon)$ is polarity function given by equation: $f(\varepsilon) = (\varepsilon - 1)/(\varepsilon + 2)$. The upper part of table represents the calculation results for 3AF molecule optimized in the ground (S_0) state while the lower part shows the results for its geometry optimized in the excited (S_1) state. Abbreviations of solvents used in PCM model is the following: HEX, *n*-hexane; DEE, di-ethyl eter; EtAc, ethyl acetate; DCM, dichloro methane; ACN, acetonitrile.

optimization are less accurate. Therefore, a steeper slope of experimental dependency relative to the theoretical results presented in Fig. 5, may imply that the real excited state dipole moment of 3AF is slightly larger than the calculated one. An increment about 2–3D in comparison to the ground state confirms a partial charge transfer character of the emissive state of 3AF.

3.3. *Lifetimes*

In the preceding sections we described the solvent effect on the calculated and experimental absorption and emission spectra. We also concluded that the target 3AF fluorophore may manifest a partial charge separation in the excited state but so far the rate constants for this process have not yet been discussed.

In this chapter, based on theoretical calculations, we formulate a hypothesis that explains the observed experimental results.

In Fig. 6, the experimental reciprocals of lifetimes, i.e. excited state deactivation rate constants ($k = 1/\tau$) *versus* polarity function $f(\varepsilon)$ are depicted. The rate constants are the sum of all the rate constants and describe the radiative and nonradiative processes

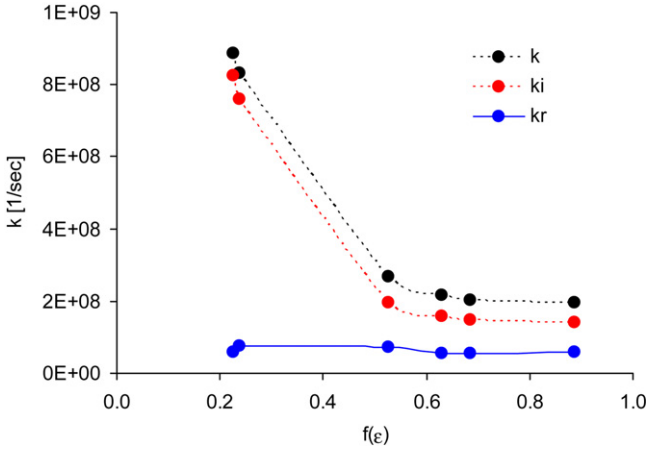

Fig. 6. The deactivation rate constants of the S_1 state of 3AF in solvents of various polarity *versus* polarity function [$f(\varepsilon)$]; The highest line shows the rate constants that were calculated from the estimated quantum yields and lifetime measurements (see Table 2). The lower line – experimental overall rate constants ($k = k_f + k_{nr}$) and the lowest line – the calculated data of kr = k_f, where $k_f = \nu_{fl}{}^2 * f/1.5$, with ν_{fl}, fluorescence maximum; and f, oscillator strength).

($k = k_f + k_{nr}$). Interestingly, they preserve more or less a constant value in polar environments while in weakly polar media they increase rapidly.

Since the appropriate data concerned with a non-typical behavior of 3AF in the solvents used are unknown, we suppose that the reason for so high deactivation rate constants may origin from one of the two radiationless processes; internal conversion (k_{IC}) or intersystem crossing (k_{ISC}).

Keeping in mind that the overall nonradiative rate constant (k_{nr}) is the sum of k_{IC} and k_{ISC} ($k_{nr} = k_{IC} + k_{ISC}$), the singlet–triplet state distribution in the function of solvent polarity was thoroughly analyzed. In a search for the appropriate process causing a sudden increase in the radiationless deactivation rate constant of excited 3AF, additional theoretical calculations have been performed. The results of calculations obtained for the various polar solvents are presented in Fig. 7. They show that changes of the solvent polarity may tune the change of the excited state energy.

It is particularly interesting to observe that with the increase of solvent polarity the energy of the S_1 state (the state of the partial CT nature) drops down to a much greater extent than the energy of the closely lying the T_2 triplet state. This triplet likewise to the S_1 state is of the $\pi\pi^*$ character.

As seen, the T_2 state in the gas phase is lying below the S_1 state and being fairly well separated. Hence, the ISC channel in this case

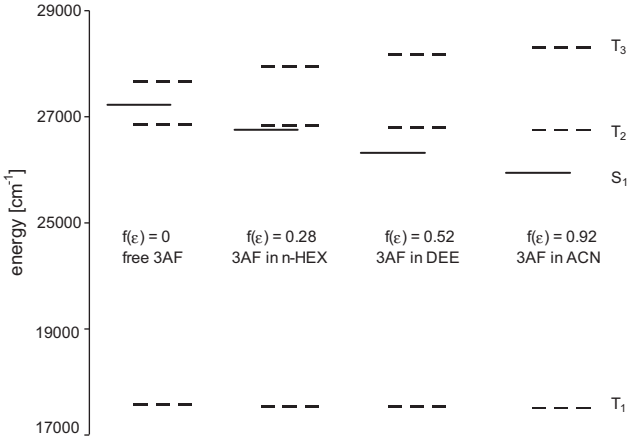

Fig. 7. The TDDFT distribution of the triplet and singlet states of 3AF in solvents of various polarity (the solvent effect in PCM model).

is unlikely to be active (we have no experimental data on this subject). However, in solvents of a low polarity [in Fig. 7, $f(\varepsilon) = 0.28$] both these states are almost isoenergetic [$E(T_2) = E(S_1)$] what may suggest a high probability of ISC process to occur. Moreover, we find that in highly polar solvents there is an inversion of states [$E(T_2) > E(S_1)$] and the intersystem crossing process becomes again virtually impossible.

The 3AF does not however emit phosphorescence and so our hypothesis is based exclusively on the calculations. The triplet–triplet transient absorption experiment would be necessary to confirm it.

4. Conclusions

The 3AF molecule has been studied by the spectroscopic and computational methods involving the geometry optimization both in the ground and in electronic excited state. Surprisingly, the system does not form a hydrogen bond involving the amino proton and the oxygen of the carbonyl group of the benzopyrone ring. The calculation results are consistent with the experiment both in terms of the energy of states, and with respect to the solvatochromic shift values.

The TDDFT eigenvectors analysis has allowed us to assign the experimental absorption maxima. We have found that the low-energy experimental absorption band in iso-octane at 27855 cm^{-1} ($S_0 \rightarrow S_1$ transition) is described by the ($\pi \rightarrow \pi^*$) HOMO $\rightarrow$ LUMO electronic configuration (27231 cm^{-1}) showing a partial charge transfer character. On excitation, the electronic density shifts from the electron rich amino group to electron deficient carbonyl group and the aromatic ring of the chromone system.

An interesting hypothesis has also been made regarding the high value of the nonradiative rate constants of excited 3AF found in iso-octane and hexane.

The lifetime measurements in function of solvent polarity and the energy calculations of the singlet and triplet state distribution in different environments (PCM model) allow us to suppose that in weakly polar solvents (isoenergetic S_1 and T_2 states) the intersystem crossing (ISC) may be a dominating excited state nonradiative relaxation process.

In polar solvents, on the other hand, due to the inversion of the S_1 and T_2 states and the large energy gap between them, the internal conversion may prevail.

Acknowledgements

We acknowledge help of Mr. Łukasz Liszkowski in some measurements of the room temperature fluorescence spectra and the lifetimes.

We thank the Interdisciplinary Center for Mathematical and Computational Modeling in Warsaw (Grant no. G32-10) and partially the Wrocław Center for Networking and Supercomputing (Grant no. 61) for the use of its computational facilities. Ł.W. also greatly acknowledges the financial support of the Ministry of Science and High Education, Poland (Grant no. **N N204 131338**).

References

[1] B. Havsteen, Biochem. Pharmacol. 32 (1983) 1141–1148.
[2] P. Nijveldt, E. Nood, D.E.C. Hoorn, P.G. Boelens, K. Norren, P.A.M. Leeven, Am. J. Clin. Nutr. 74 (2001) 418–425.
[3] B. Kośmider, E. Osiecka, Drug Dev. Res. 63 (2004) 200–211.
[4] Y. Sorata, U. Takahama, M. Kimura, Photochem. Photobiol. 48 (1988) 195–199.
[5] (a) D. McMorrow, M. Kasha, J. Phys. Chem. 88 (1984) 2235–2243;
(b) P.K. Sengupta, M. Kasha, Chem. Phys. Lett. 68 (1979) 382–385;
(c) M. Itoh, K. Hasegawa, Y. Fujiwara, J. Am. Chem. Soc. 108 (1986) 5853–5857;
(d) S.M. Ormson, R.G. Brown, F. Volmer, W. Rettig, J. Photochem. Photobiol. A 81 (1994) 65–72.
[6] P.T. Chou, Y.C. Chen, W.S. Yu, Y.M. Cheng, Chem. Phys. Lett. 340 (2001) 89–97.
[7] A.D. Roshal, J.A. Organero, A. Douhal, Chem. Phys. Lett. 379 (2003) 53–59.
[8] A.J.G. Strandjord, P.F. Barbara, J. Phys. Chem. 89 (1985) 2355–2361.
[9] N. Chattopadhyay, M. Baroso, C. Serpa, L.G. Arnaut, S.J. Formosinho-Chem, Phys. Lett. 387 (2004) 236–262.
[10] (a) P.T. Chou, M.L. Martinez, J.H. Clements, J. Phys. Chem. 97 (1993) 2618–2622;
(b) P.T. Chou, M.L. Martinez, J.H. Clements, Chem. Phys. Lett. 204 (1993) 395–399.
[11] (a) T.C. Swinney, D.F. Kelley, J. Chem. Phys. 99 (1993) 211–222;
(b) F. Parsapour, D.F. Kelley, J. Phys. Chem. 100 (1996) 2791–2798.
[12] S.M. Ormson, R.G. Brown, F. Vollmer, W. Rettig, J. Photochem. Photobiol. A 81 (1994) 65–72.
[13] P.-T. Chou, S.-C. Pu, Y.-M Cheng, W.-S Yu, Y.-C Yu, f.-T Hung, W.-P Hu, J. Phys. Chem. 109 (2005) 3777–3787.
[14] S.M. Beyhan, A.W. Gotz, F. Ariese, L. Visscher, C. Gooijer, J. Phys. Chem. A 115 (2011) 1493–1499.
[15] B. Żurowska, A. Erxleben, Ł. Glinka, M. Łęczycka, E. Zyner, J. Ochocki, Inorg. Chim. Acta 362 (2009) 739–744.
[16] G.A. Crosby, J.N. Demas, Measurements of photoluminescence quantum yields, J. Phys. Chem. 75 (1971) 991–1024.
[17] M.J. Frisch, et al., Gaussian 09 Revision B. 01, Gaussian, Inc., Wallingford, CT, 2010.
[18] L. Onsager, J. Am. Chem. Soc. 58 (1936) 1486–1493.